Supplementary Information

Compositional Control of the Effective Magnetic Anisotropy in Mn and Co Substituted Spinel Nanoparticles

[1]Alexander Malaj, [1]Cathryn Leies, [1]Zachary Caprow, [2]Venkata Rohit Punyapu, [3]Ehimen A. Odion, [2]Rachel Getman, [4]Karen L Livesey, [1]Suvra S. Laha* and [1,3] O. Thompson Mefford*

[1] Department of Materials Science and Engineering, Clemson University, Clemson, SC 29634, USA

[2] William G. Lowrie Department of Chemical and Biomolecular Engineering, The Ohio State University, Columbus, OH 43210, USA

[3]Department of Chemistry, Clemson University, Clemson, SC 29634, USA

[4]School of Information and Physical Sciences, University of Newcastle, University Drive, Callaghan, 2308, NSW, Australia.

*Corresponding authors: slaha@clemson.edu; mefford@clemson.edu

X-ray Diffraction (XRD) analysis

X-ray diffraction (XRD) measurements were carried out using a Rigaku MiniFlex 600 benchtop diffractometer and a Rigaku SmartLab diffractometer. The XRD pattern for MM-1 was acquired using the MiniFlex 600 system. For subsequent samples (MM-2 to MM-7), measurements were performed using the Rigaku SmartLab diffractometer to obtain higher-resolution data. All measurements were conducted using Cu K_α radiation (λ = 1.54 Å). The XRD plots are shown in Fig. S1.

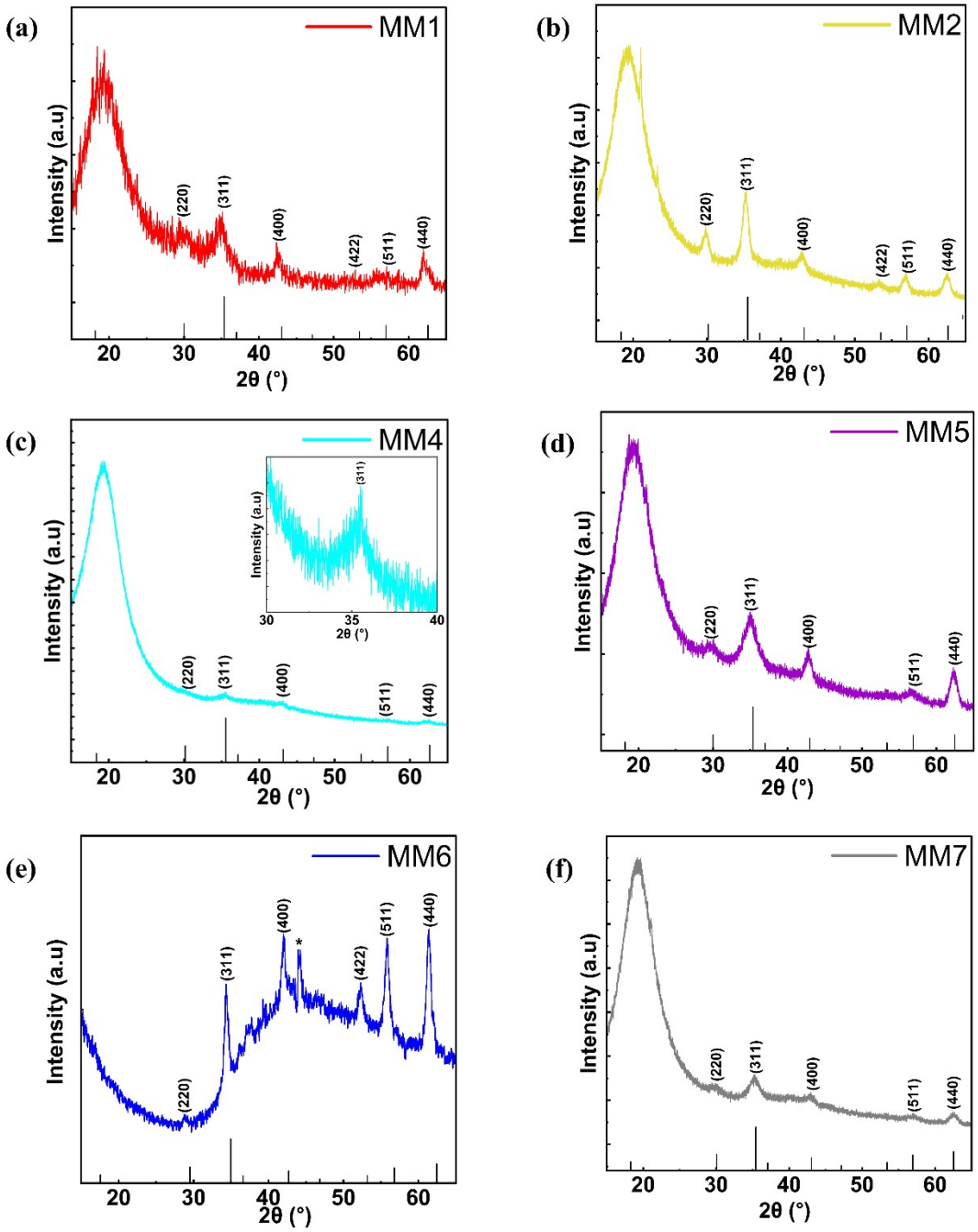

Fig. S1. X-ray diffraction (XRD) patterns of samples (a) MM-1, (b) MM-2, (c) MM-4, (d) MM-5, (e) MM-6, and (f) MM-7. All samples exhibit diffraction peaks corresponding to a cubic spinel ferrite structure. The peak positions closely match those of the magnetite crystal phase (JCPDS Card No. 85-1436), indicating that the synthesized nanoparticles adopt a typical spinel ferrite lattice despite the presence of multiple transition metal cations. A broad hump observed at low diffraction angles (~15^{o}- 25 °) suggests the presence of an amorphous background, most likely associated with residual organic species in the thermal decomposition synthesis route. In MM6, an additional diffraction peak (marked with asterisks) is observed, which may originate from minor

impurity phases. Overall, the diffraction patterns confirm the formation of spinel ferrite nanoparticles across the sample series. The XRD pattern of MM-3 (not shown) did not display any distinct diffraction peaks, suggesting a largely amorphous or poorly crystalline phase.

Table S1. Table providing the mean and standard deviations for each nanoparticle series. The means and standard deviations for the volumes were calculated using a log-normal distribution. The mean blocking temperatures and the mean DC K_{eff} values are also included.

Sample	Mean diameter d (nm)	Standard dev diameter (nm)	Mean volume V (nm^3)	Standard dev volume (nm^3)	Mean blocking temp T_B (K)	Mean DC K_{eff} (kJ/m^3)
MM-1	10.4	1	606	178	134	77
MM-2	10.6	1.6	667	310	204	130
MM-3	10.5	1.3	634	240	112	61
MM-4	9.58	1.8	510	306	85	57
MM-5	10	1.56	566	278	71	44
MM-6	8.8	2.96	492	648	78	55
MM-7	8.42	1.1	328	133	38	40